Holography for quark-gluon plasma formation in heavy ion collisions

Irina Aref'eva[*][†]

Steklov Mathematical Institute, Russian Academy of Science,
Gubkin str. 8, 119991, Moscow, Russia
E-mail: `arefeva@mi.ras.ru`

For the last decade, the AdS/CFT correspondence, which appeared as a formal duality between the $N = 4$ super Yang–Mills theory and quantum gravity in the AdS background, has become a powerful tool for studying various properties of real physical systems in the strong-coupling limit. An important branch of these investigations is the analysis of the quark–gluon plasma from the standpoint of AdS holography.

We review a particular application of the AdS/CFT correspondence to the analysis of the thermalization of matter and entropy production after the collision of relativistic heavy ions. The appearance of the quark-gluon plasma after the heavy-ion collision in dual terms is described as formation of a black hole. We discuss mainly two holographic dual models of thermalization.

In the first one colliding ions are described by gravitational shock waves in AdS and the formation of the black hole is provided of the formation of a trapped surface. In the dual language, the multiplicity of the ion collision process is estimated as the area of the trapped surface. The charged gravitational shock waves correspond to nonzero chemical potential and a nonzero chemical potential reduces the multiplicity.

The second holographic model for quark-gluon plasma formed in the heavy ion collisions is based on AdS-Vaidya model. In the model the process of thermalization is described also as formation of the black hole in AdS space while dethermalization process, related with the freeze-out, as the black hole evaporation due to the Hawking radiation that is modeled by the Vaidya metric with a negative mass. In this model the thermalization takes place only at small scales and absent in the infrared region.

7th Conference Mathematical Methods in Physics - Londrina 2012,
16 to 20 April 2012
Rio de Janeiro, Brazil

---

[*]Speaker.

[†]A footnote may follow.

1. Introduction

There are many attempts to describe the process of heavy ion collisions and quark-gluon plasma formation (QGP) [1]-[9] in the QCD framework [10]-[12]. One of difficulties is that one has to compute the time depended correlation functions in the strong coupling regime since the QGP is a strong coupling system.

In the recent years a powerful approach to QGP is pursued which is based on a holographic duality between the strong coupling quantum field in d-dimensional Minkowski space and classical gravity in $d+1$-dimensional anti-de Sitter space (AdS) [13, 14, 15]. In particular, there is a considerable progress in the holographic description of equilibrium QGP [16]. The holographic approach is also applied to non-equilibrium QGP. Within this holographic approach thermalization is described as a process of formation of a black hole in AdS.

In these lectures we are going to describe applications of the holographic approach to the thermalization problem in heavy ion collisions.

2. Quark-Gluon Plasma - a new state of matter

2.1 Main characteristics of QGP

The quark-gluon plasma is a state of matter formed from deconfined quarks, antiquarks, and gluons at high temperature. We know that quarks and gluons are described by QCD. In QCD we have quark confinement and asymptotic freedom.

It is known (mainly due to lattice calculations, [17]) that if the temperature T increases, or the density nuclear matter ε increases then nuclear matter undergoes to a phase transition to deconfined phase. The temperature-chemical potential phase diagram of QCD is not well known either experimentally or theoretically. The chemical potential μ is a measure of the imbalance between quarks and antiquarks in the system. A commonly conjectured form of the phase diagram, temperature T vs quark chemical potential μ, is shown in Fig.1, see for example [11].
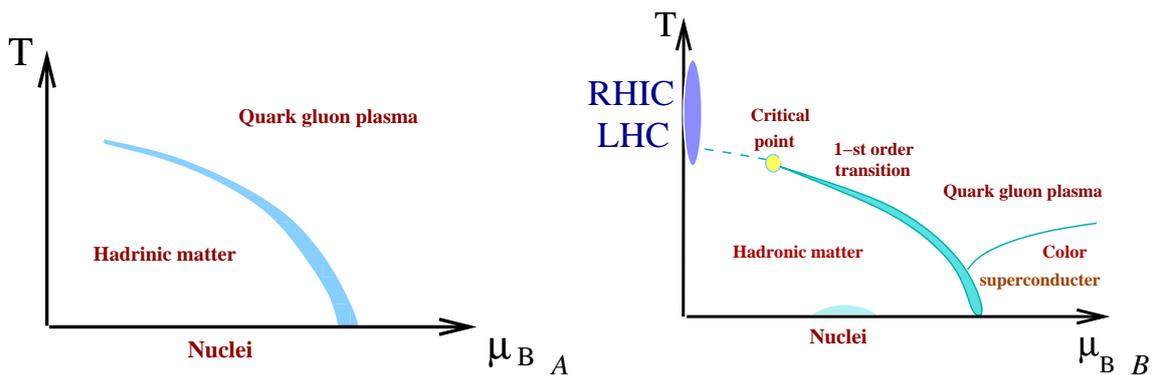
Figure 1: A. Oversimplified QCD phase diagram. B. QCD phase diagram with more details.
.

The phase transition is not sharp and it is supposed to be the 1-st order. At a critical point $T \sim 200$ MeV and $\varepsilon \sim 1 GeV/fm^3$ (here ε is the energy density). Ordinary nuclear matter in this

diagram is at μ = 310 MeV and T close to zero. If we increase the quark density, i.e. increase μ, keeping the temperature low, we go into a phase of more and more compressed nuclear matter (neutron stars).

Above the blue smeared line there is a transition to the quark-gluon matter, where colored particles are free to propagate over macroscopic distances, giving rise to a non-trivial collective dynamics. At ultra-high densities one expects to find the phase of color-superconducting quark matter. In ultra-relativistic heavy ion collisions one studies this matter in the regime of extreme energy density. In Fig.1 the typical values of μ and T in heavy-ion in heavy-ion collisions are shown by a blue region.

2.2 QGP in Heavy Ion Collision and Early Universe

One of the fundamental questions in physics is: what happens to matter at extreme densities and temperatures, $T \sim 10^{12}$ K, as may have existed in the first microseconds, $t \sim 10^{-5}$ sec, after the Big Bang. One can say that one of the aim of heavy-ion physics is to collide nuclei at very high energies and create such a state of matter in the laboratory.

One can think of a heavy ion collision as a "little bang", replaying the history of the big bang in a small volume [18]. In the right part of Fig.2 we plot the collision of two Lorentz contracted nuclei. At $t = 0$ when these contracted nuclei are coincident and the entire energy of the two nuclei is found within a smaller volume, the density becomes very higher. Just after collision the quarks and gluons undergo multiple interactions and the system will thermalize and form the QGP. Elliptic flow data indicate that by ~ 1 fm/c after the collision, matter is flowing collectively like a fluid in local equilibrium [1]-[3], see also the recent review [9] and refs therein. Then, as in the early universe, the hot and dense system created in a heavy ion collision will expand and cool down and eventually it becomes enough dilute to hadronize.

The analogue of the cosmological epoch of nucleosynthesis, the time at which the composition of the final state hadron gas stops changing, in heavy ion collisions is a kinetic freeze-out.

3. Physics of Heavy Ions Collisions

In a heavy ion collision experiment, large nuclei are collided at an ultra-relativistic center of mass energy. At the Brookhaven Alternating Gradient Synchrotron (AGS), started in the 1990's, the s-parameter per one nucleon is $\sqrt{s_{NN}} = 4.75 GeV$, at the CERN Super Proton Synchrotron (SPS), $\sqrt{s_{NN}} = 17.2 GeV$, at the Brookhaven Relativistic Heavy-Ion Collider (RHIC), $\sqrt{s_{NN}} = 200 GeV$ and at the LHC collider at CERN, $\sqrt{s_{NN}} = 2.76 TeV$. At RHIC the ions of Au are collided and at LHC the ions of Pb are collided. Schematically the picture of heavy ion collisions is presented in Fig.2.

There are strong experimental evidences that RHIC or LHC have created some medium, see Fig.3, which behaves collectively [1]-[9]:

- modification of particle spectra (compared to p+p),

- high p_T -suppression of hadrons,

- jet quenching, i.e. behavior if R_{AA},
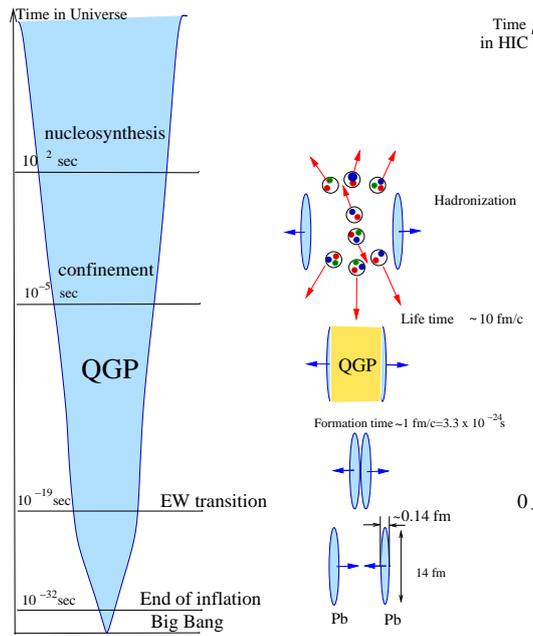
Figure 2: QGP in Heavy Ion Collision and in Early Universe.

.

- elliptic flow

- suppression of quarkonium production,

- temperature measurement by direct photons,
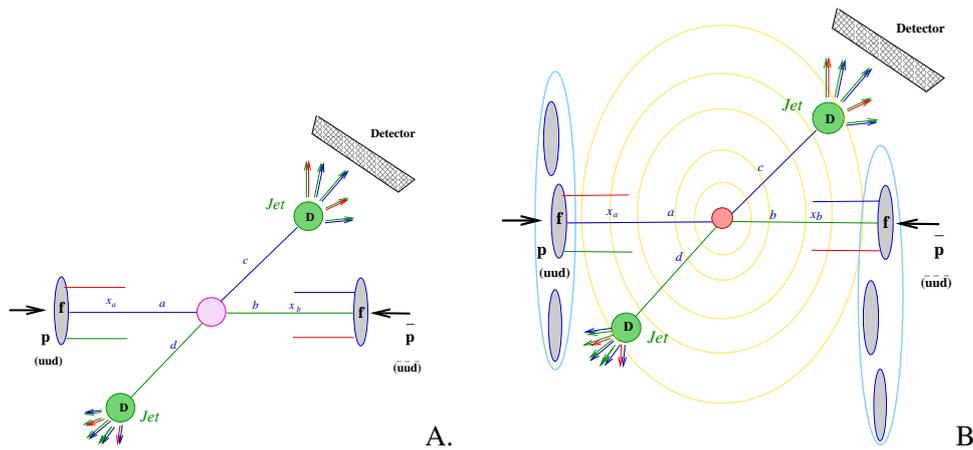
Figure 3: A.Perturbative QCD factorization in hadronic collisions. B. Perturbative QCD factorization in heavy ion collisions. Yellow waves indicate the presence of a media.

It is now widely appreciated that the experiments at the RHIC [1, 2] and at the LHC[3] produce the quark-gluon plasma that behaves as a strongly coupled fluid, but not as a weakly coupled gas of quarks and gluons [4, 5]. This means that we cannot use perturbative methods to describe QGP. The

lattice QCD is also inapplicable since it is not well suited for studying real-time phenomena. This has provided a strong motivation for understanding the dynamics of strongly coupled non-Abelian plasmas through the gauge/string duality [13, 14, 15].

In the process of collision of two ions one observes a rapid local thermalization of the system of partons with further expansion and cooling of system which leads to hadronization and multiple production of particles. Experiments indicate to a very short thermalization time, $\tau_{therm} \sim 1$ fm/c for the quark-gluon plasma(QGP) formed in heavy ion collisions, while the freeze-out time is of order 20 fm/c [1, 10, 5, 12, 8, 20].

In more details, the time schedule of the process is the following. Up to a time ~ 0.02 fm/c "hard" processes take place and they are responsible for "hard" particles, which can be observed at detectors. Up to a time ~ 0.2 fm/c "semi-hard" processes take place and they produce the most of the "multiplicity" in the final state. Then at the thermalization time of order $\tau_{therm} \sim 1$ fm/c the system reaches a local thermal equilibrium state, called QGP. After that the evolution of QGP is described by equations of hydrodynamics and after the time of order $\tau_{hadr} \sim 10$ fm/c, when due to the separation of the colliding ions the temperature becomes lower than the deconfinement temperature, a hot hadron gas is formed. Upon the further expansion and cooling, around the freeze-out time $\tau_{det} \sim 20$ fm/c, the density of the hadron gas become sufficiently low and the system decays into free hadrons, which can be observed at detectors. Therefore in experiments on heavy ion collisions there is the following hierarchy of time scales:

$$\tau_{therm} < \tau_{hydro} < \tau_{hadr} < \tau_{fr-out}. \tag{3.1}$$

One can interpret the freeze-out time as the dethermalization time $\tau_{fr-out} \sim \tau_{det}$ [21]. There are many attempts to describe the process of heavy ion collisions and QGP formation in the QCD framework. One of difficulties is that one has to compute the time depended correlation functions in the strong coupling regime since the QGP is a strong coupling system [10]. In the recent years a new approach to non-equilibrium QGP has been initiated. This approach, also uses a holographic duality between the strong coupling quantum field in d-dimensional Minkowski space and classical gravity in $d+1$-dimensional anti-de Sitter space (AdS). Within this holographic approach thermalization process is described as a process of formation of a black hole in AdS.

4. Dual description of QGP as a part of Gauge/string duality

The Gauge/Gravity duality [13, 14, 15] gives a correspondence between the quantum gauge field theory in 4-dimensional Minkowski space-time and the 5-dimensional supergravity (weak curvature) approximation of the 10-dimensional string theory. Or in others words, the properties of the gauge theory in (physical) Minkowski space in 3+1 dimensions are in one-to-one relation with properties of the bulk theory. The best known example of such theories is N = 4 super Yang-Mills, a superconformal field theory with matter in the adjoint representation of the gauge group $SU(N_c)$ which is dual to the IIB superstring theory on $AdS_5 \times S^5$.

However, there is not yet found a gravity dual to QCD. Differences between N = 4 SYM and QCD are less significant, when quarks and gluons are in the deconfined phase (because of the conformal symmetry at the quantum level N = 4 SYM theory does not exhibit confinement.)
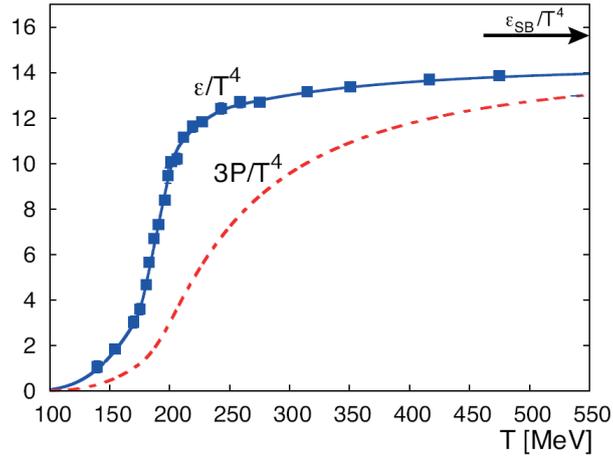
Figure 4: Results [19] from a lattice calculation of QCD thermodynamics with physical quark masses ($N_f = 3$, with appropriate light and strange masses). Energy density ε/T^4 (full curve) and pressure $3P/T^4$ (dashed curve) as a function of temperature T from lattice calculations. The arrow indicates the Boltzmann limit of the energy density. Figure is taken from Ref. [9].

Lattice calculations [19] show that QCD exhibits a quasi-conformal behavior at temperatures T >300 MeV and the equation of state can be approximated by $\varepsilon = 3$ p (a traceless conformal energy-momentum tensor), see Fig.4.

The above observations, have motivated to use the AdS/CFT correspondence as a tool to get non-perturbative dynamics of QGP.

There is the considerable success in description of the static quark-gluon plasma, in particular in the evaluation of η/s [22]-[25], see also paper[26] about discussion of violation of the holographic bulk viscosity bound.

4.1 Mapping of parameters

- Gauge theory has two parameters:

    - Coupling constant (elementary charge) g
    - Number of colors N_c

    Whether the theory is weakly or strongly coupled depends on $g^2 N_c$

- String theory side has three parameters

    - String length l_s, i.e. a typical size of string vibrations
    - String coupling g_{st}
    - Curvature of space R

Mapping between the parameters is:

$$g^2 = 4g_{st} \tag{4.1}$$

$$g^2 N_c = \frac{R^4}{l_s^4} \tag{4.2}$$

Strong coupling limit in field theory $g^2 N_c >> 1$,

$$\text{string length} << \text{curvature radius} \tag{4.3}$$

and we can use Einstein gravity instead of string theory.

4.2 AdS/CFT in simple examples

4.2.1 AdS/CFT in Euclidean space

For simplicity, we shall consider here the correspondence between the d-dimensional quantum conformal Euclidean field theory and classical gravity on AdS$_D$, $D = d + 1$. The Euclidean version of the AdS$_D$ metric has the form

$$ds^2 = \frac{R^2}{z^2}(d\tau^2 + d\vec{x}^2 + dz^2), \tag{4.4}$$

which is a solution to the Einstein equations. In the AdS/CFT correspondence, the d-dimensional quantum field theory lives on the boundary of the AdS$_D$ space at $z = 0$. Suppose that a bulk field ϕ is coupled to an operator $\mathscr{O}$ on the boundary in such a way that the interaction Lagrangian is $\phi \mathscr{O}$. In this case, the AdS/CFT correspondence is formally stated as the equality [14, 15]

$$\left\langle e^{\int_{\partial M} \phi_0 \mathscr{O}} \right\rangle = e^{-S[\phi_{\text{cl}}(\phi_0)]}, \tag{4.5}$$

where the left-hand side is the generating functional for correlators of in the boundary field theory (i.e. the d-dimensional conformal field theory), and the exponent on the right-hand side is the action of the classical solution to the equation of motion for ϕ in the bulk metric with the boundary condition

$$\delta S[\phi_{\text{cl}}] = 0, \quad \phi_{\text{cl}}|_{z=0} = \phi_0. \tag{4.6}$$

Let us consider as an example the scalar massless field in AdS_D. The action is given by

$$I = \frac{1}{2} \int_\varepsilon^\infty dz \int_{R^d} d\mathbf{x} \frac{1}{z^{d-1}} \sum_{i=0}^d (\partial_i \phi)^2, \qquad \mathbf{x} = (\tau, \vec{x}) \tag{4.7}$$

Here $\varepsilon > 0$ is a cut-off, see [14]. The solution to the Dirichlet problem

$$\left(\frac{\partial^2}{\partial z^2} + \sum_{i=1}^d \frac{\partial^2}{\partial x_i^2} - \frac{(d-1)}{z} \frac{\partial}{\partial z} \right) \phi = 0, \qquad \phi|_{z=0} = \phi_0(\mathbf{x}) \tag{4.8}$$

can be represented in the form

$$\phi(z, \mathbf{x}) = c z^{d/2} \int_{R^d} d\mathbf{p} e^{i\mathbf{p}\mathbf{x}} |\mathbf{p}|^{\frac{d}{2}} K_{\frac{d}{2}}(|\mathbf{p}|z) \tilde{\Phi}_0(\mathbf{p}), \tag{4.9}$$

where $K_{\frac{d}{2}}(y)$ is the modified Bessel function. By integrating by parts, one can rewrite (4.7) as

$$I = -\frac{1}{2} \int_{R^d} d\mathbf{x} \left. \frac{\phi \partial_z \phi}{z^{d-1}} \right|_{z=\varepsilon} \tag{4.10}$$

Using the asymptotic expansion of the modified Bessel function one gets a regularized expression for the action. For $d = 4$ one has for $z \to 0$

$$\Phi(z,\mathbf{x}) = C \int_{R^4} d\mathbf{p} e^{i\mathbf{px}} [2 - \frac{1}{2}(z|\mathbf{p}|)^2 - \frac{(z|\mathbf{p}|)^4}{8} \log \frac{z|\mathbf{p}|}{2} + c(z|\mathbf{p}|)^4 + \ ... \ ] \tilde{\Phi}_0(\mathbf{p}). \qquad (4.11)$$

The action (4.10) for $\varepsilon \to 0$ behaves as

$$I = C \int_{R^4} d\mathbf{p} |\tilde{\Phi}_0(\mathbf{p})|^2 [-\frac{1}{\varepsilon^2}|\mathbf{p}|^2 - \frac{|\mathbf{p}|^4}{2} \log \frac{\varepsilon|\mathbf{p}|}{2} + c_1 |\mathbf{p}|^4 + \ ... \ ]. \qquad (4.12)$$

The renormalized action

$$I_{ren} = \int_{R^4} d\mathbf{p} |\tilde{\Phi}_0(\mathbf{p})|^2 [a p^4 \log |\mathbf{p}|^2 + b |\mathbf{p}|^4]. \qquad (4.13)$$

can be written in term of distribution $|\mathbf{x} - \mathbf{y}|^{-\mathbf{2d}}$ [27],

$$I_{ren} = \int_{R^d} \frac{\Phi_0(\mathbf{x}) \Phi_0(\mathbf{y})}{|\mathbf{x} - \mathbf{y}|^{2d}} d\mathbf{x} d\mathbf{y} \qquad (4.14)$$

for $d = 4$, since, according to [28],

$$\widetilde{|\mathbf{x}|^{-8}} = a p^4 \log |\mathbf{p}| + b |\mathbf{p}|^4. \qquad (4.15)$$

4.2.2 BHAdS/TCFT

To compute the Matsubara correlator at finite temperature, one uses (4.5) with a replacement of the metric (4.4) by the following metric

$$ds^2 = \frac{R^2}{z^2} \left(f(z) d\tau^2 + d\vec{x}^2 + \frac{dz^2}{f(z)} \right), \qquad (4.16)$$

where

$$f(z) = 1 - z^d / z_H^d \qquad (4.17)$$

and

$$z_H = (4\pi T/d)^{-1}, \qquad (4.18)$$

and T is the Hawking temperature. The Euclidean time coordinate τ is periodic, $\tau \sim \tau + T^{-1}$, and z runs between 0 and z_H.

The Minkowski version of the AdS/CFT could be the equivalence

$$\langle e^{i \int_{\partial M} \phi_0 \mathcal{O}} \rangle = e^{i S_{cl}[\phi]}. \qquad (4.19)$$

However, this conjecture does nor work straitforwardly [29]. In the Euclidean version, the classical solution ϕ is uniquely determined by its value ϕ_0 at the boundary $z = 0$ and the requirement of regularity at the horizon $z = z_H$. Therefore, Euclidean correlators obtained by using the correspondence are unique. In the Minkowski space, the requirement of regularity at the horizon is insufficient to select a solution. This fact is related with the multitude of real-time Green's functions (Feynman,

retarded, advanced) in finite-temperature field theory. The classical action is reduced to the surface term

$$S = \int \frac{d^4k}{(2\pi)^4} \phi_0(-k) \mathscr{F}(k,z) \phi_0(k) \Big|_{z=z_B}^{z=z_H}, \tag{4.20}$$

and a viable recipe is

$$G^R(k) = -2\mathscr{F}(k,z) \Big|_{z_B}, \tag{4.21}$$

see the original paper [29] for the definition of $\mathscr{F}$ and for details.

4.2.3 AdS/CFT with geodesic approximation

It is more convenient to follow [30] and to observe that the Green function for space-like separated points can be computed via a path integral as

$$\langle \mathscr{O}_\Delta L(t,\vec{x}) \mathscr{O}_\Delta L(t',\vec{x}') \rangle = \int \mathscr{DP} \, e^{i\Delta L(\mathscr{P})} \approx \sum_{\text{geodesics}} e^{-\Delta \mathscr{L}}. \tag{4.22}$$

Here the path integral is over all paths that begin and end at the boundary points $(t,\vec{x})$ and $(t',\vec{x}')$, $L(\mathscr{P})$ is the proper length of the path. $L(\mathscr{P})$ is imaginary for space-like trajectories. The second expression means a saddlepoint approximation to the path sum as a sum over geodesics. Here $\mathscr{L}$ is the real length of the geodesic between the boundary points. This approximation is effective when $\Delta \gg 1$.

In $d = 2$ case it is easy to check explicitly that in AdS space, this formula gives the correct conformally invariant equal-time two point function of the renormalized operator

$$\langle \mathscr{O}_\Delta^{\text{ren}}(t,-\ell/2) \mathscr{O}_\Delta^{\text{ren}}(t,\ell/2) \rangle = e^{-\Delta \ln \ell^2}. \tag{4.23}$$

Indeed, let us consider the Lorentz version of the metric (4.16) for $d = 2$, $R = 1$ in (r,t,x)-coordinates, $r = 1/z$,

$$ds^2 = -f(r)\,dt^2 + \frac{1}{f(r)}\,dr^2 + r^2\,dx^2 \tag{4.24}$$

Introducing as usual the conjugated momenta along the geodesic

$$P^i \equiv \dot{X}^i, \; X^i = \{t,r,x\}, \; P^i = \{p^t, p^r, p^x\} \equiv \{\dot{t}, \dot{r}, \dot{x}\}, \; P_i = g_{ik} P^k, \; P_i = \{p_t, p_r, p_x\} \tag{4.25}$$

we get

$$p_t = -f\dot{t}, \; p_r = \frac{1}{f}\dot{r}, \; p_x = r^2 \dot{x} \tag{4.26}$$

Two of these conjugated momenta, p_t and , p_x conserve and we denote them as

$$E \equiv -p_t, \; J \equiv p_x \tag{4.27}$$

The affine parameter condition

$$g_{\mu\nu} \dot{X}^\mu \dot{X}^\nu = 1, \tag{4.28}$$

leads to

$$\dot{r}^2 = f + E^2 - \frac{J^2 f}{r^2} \tag{4.29}$$

9

or

$$r'^2 = \frac{r^4 f}{J^2} + \frac{r^4 E^2}{J^2} - f r^2 \tag{4.30}$$

Here the dot means the derivative in respect to the affine parameter, meanwhile the prime denote the derivative in respect to x along the geodesic.

In the case of equal time geodesic $\dot{t} = 0$ and therefore, $E = 0$. In the case of AdS_3, $f(r) = r^2$ and we have a turning point r_* on a geodesic

$$r_* = |J| \tag{4.31}$$

One can calculate the proper length $\mathscr{L}$ and the expansion ℓ along x,

$$\mathscr{L}_{AdS} = \int d\tau = \int dr/\dot{r} = 2 \int_{r_*}^{r_\infty} \frac{dr}{\sqrt{r^2 - p_x^2}} = 2 \log(r + \sqrt{r^2 - p_x^2}) \Big|_{r_*}^{r_\infty} = 2\ln(2r_\infty) - 2\ln p_x,$$

$$\ell_{AdS} = \int dx = \int dr/r' = 2 \int_{r_*}^{r_\infty} \frac{dr}{r^2 \sqrt{\frac{r^2}{p_x^2} - 1}} = \frac{2}{r} \sqrt{r^2/p_x^2 - 1} \Big|_{r_*}^{r_\infty} = \frac{2}{p_x}. \tag{4.32}$$

It is clear that

$$\mathscr{L}_{AdS} = 2\ln(2r_\infty) + 2\ln \frac{l_{AdS}}{2}. \tag{4.33}$$

The geodesic length $\mathscr{L}_{AdS}$ diverges due to contributions near the AdS boundary. Therefore, we define a renormalized length $\delta\mathscr{L} \equiv \mathscr{L} - 2\ln(r_\infty)$, in terms of the cut-off r_∞, by removing the divergent part of the geodesic length in pure AdS (compare with the action renormalization considered in [27]). The renormalized equal-time two-point function is

$$\langle \mathcal{O}_\Delta^{\mathrm{ren}}(t,\mathbf{x}) \mathcal{O}_\Delta^{\mathrm{ren}}(t,\mathbf{x}') \rangle \sim e^{-\Delta\delta\mathscr{L}} = e^{-\Delta\ln\ell^2}, \tag{4.34}$$

that obviously coincides with (4.23).

4.2.4 BHAdS/TCFT with geodesic approximation

As in the previous subsection one can easily calculate the length of an equal time geodesic in BHAdS. The metric is given by (4.24) witt

$$f = r^2 - 1 \tag{4.35}$$

In this case $E = 0$ and the turning point is also defined as $r_* = |J|$. One can calculate the proper length $\mathscr{L}$ and the expansion ℓ along x,

$$\mathscr{L}_{BHAdS} = \int d\tau = \int \frac{dr}{\dot{r}} = 2 \int_{r_*}^{r_\infty} \frac{r\,dr}{\sqrt{(r^2-1)(r^2-J^2)}} = 2\log(r + \sqrt{r^2-J^2}) \Big|_{r_*}^{r_\infty} = 2\ln(2r_\infty) - \ln(p_x^2 - 1),$$

$$\ell_{BHAdS} = \int dx = \int \frac{dr'}{r} = 2 \int_{r_*}^{r_\infty} \frac{dr}{r\sqrt{(r^2-1)(\frac{r^2}{J^2}-1)}} = 22 \operatorname{arctanh} J + i\pi. \tag{4.36}$$

One could find the relation,

$$\mathscr{L}_{BTZ} = 2\log(2r_\infty) + 2\log\left(\sinh\left(\frac{\ell_{BTZ}}{2}\right)\right). \tag{4.37}$$

and using the notion of renormalized length we get

$$\delta \mathscr{L}_{BTZ} = 2\ln\left(\sinh\left(\frac{\ell_{BTZ}}{2}\right)\right). \tag{4.38}$$

This answer can be understand from the CFT side in the following way. The two-point function of a scalar operator $\mathscr{O}(z,\bar{z})$ in $2d$ CFT is fixed by the conformal invariance up to a normalization constant:

$$\langle \mathscr{O}(z_1,\bar{z}_1)\mathscr{O}(z_2,\bar{z}_2)\rangle = \frac{C_{12}}{(z_1-z_2)^{2h_L}(\bar{z}_1-\bar{z}_2)^{2h_R}}. \tag{4.39}$$

To find the expression for the correlator at finite temperature T, one considers a conformal map $w = \ln(z)/2\pi T$ from the infinite plane to the cylinder with circumference $L = 1/T$. The correlator (4.39) becomes

$$\langle \mathscr{O}(w_1,\bar{w}_1)\mathscr{O}(w_2,\bar{w}_2)\rangle = \frac{C_{12}(\pi T)^{2h_L}(\pi T)^{2h_R}}{\sinh^{2h_L}[\pi T(w_1-w_2)]\sinh^{2h_R}[\pi T(\bar{w}_1-\bar{w}_2)]}. \tag{4.40}$$

We see that for the case $w_1 = \ell/2$, $w_2 = -\ell/2$, and $h_L = h_R = \Delta/2$ this answer reproduces the geometrical answer for the case of $2\pi T = 1$.

4.3 Black holes and the AdS/CFT correspondence for a strongly coupled QGP

The idea of using the AdS/CFT correspondence to describe the QGP is based on the possibility of establishing a one-to-one correspondence between phenomenological/thermodynamic plasma parameters (T, E, P, and μ) and the parameters characterizing AdS$_5$ deformations. In the dual gravity setting, the source of temperature and entropy are attributed to the gravitational horizons. The relation between the energy density and temperature typical for the BH in the AdS according to [31, 32] is

$$E = \frac{3\pi^3 L^3}{16G_5}T^4. \tag{4.41}$$

In the phenomenological model of a QGP, such as the Landau or Bjorken hydrodynamic models [33, 34], the plasma is characterized by a space–time profile of the energy–momentum tensor $T_{\mu\nu}(x^\rho)$, $\mu,\nu,\rho = 0,\ldots,3$. This state has its counterpart on the gravity side as a modification of the geometry of the original AdS$_5$ metric. This follows the general AdS/CFT line: operators in the gauge theory correspond to fields in SUGRA. In the case of the energy–momentum tensor, the corresponding field is just the five-dimensional metric. It is convenient to parameterize the corresponding five-dimensional geometry as

$$ds^2 = L^2\frac{g_{\mu\nu}(x^\rho,z)dx^\mu dx^\nu + dz^2}{z^2}, \tag{4.42}$$

which is the five-dimensional Fefferman–Graham metric [35]. The flat case $g_{\mu\nu} = \eta_{\mu\nu}$ parameterizes AdS$_5$ in Poincaré coordinates. The conformal boundary of the space–time is at $z = 0$ and

$$g_{\mu\nu}(x^\rho,z) = \eta_{\mu\nu} + z^4 g^{(4)}_{\mu\nu}(x^\rho) + \ldots. \tag{4.43}$$

The AdS/CFT duality leads to the relation

$$g^{(4)}_{\mu\nu}(x^\rho) = \frac{N_c^2}{2\pi^2}\langle T_{\mu\nu}(x^\rho)\rangle, \tag{4.44}$$

where N_c is a number of colors (see [?] for a brief review).

Applying the AdS/CFT correspondence to the hydrodynamic description of the QGP is based on the fact that the energy–momentum tensor can be obtained directly from the expansion of the BH in AdS$_5$ metric (4.43) corresponding to the simple hydrodynamic model

$$\langle T_{\mu\nu} \rangle \propto g_{\mu\nu}^{(4)} = \text{diag}\left(\frac{3}{z_0^4}, \frac{1}{z_0^4}, \frac{1}{z_0^4}, \frac{1}{z_0^4} \right). \tag{4.45}$$

The AdS$_5$ BH in the Fefferman–Graham coordinates has form (4.42) with the following nonzero components of $g_{\mu\nu}(x^\rho, z)$ (see [36] and the references therein):

$$g_{00} = -\frac{(1 - z^4/z_0^4)^2}{1 + z^4/z_0^4}, \qquad g_{ii} = \left(1 + \frac{z^4}{z_0^4} \right). \tag{4.46}$$

The change of coordinates $\tilde{z} = z/(1 + z^4/z_0^4)^{1/2}$ transforms (4.42) into the standard metric form of the AdS–Schwarzschild static BH

$$\tilde{z}^2 ds^2 = -\left(1 - \frac{\tilde{z}^4}{\tilde{z}_0^4} \right) dt^2 + d\vec{x}^2 + \frac{1}{1 - \tilde{z}^4/\tilde{z}_0^4} d\tilde{z}^2, \tag{4.47}$$

where $\tilde{z}_0 = z_0/\sqrt{2}$ is the horizon location.

4.4 The chemical potential in a QGP via the AdS/CFT correspondence

The Reissner–Nordström (RN) metric in the AdS space has the form

$$ds^2 = -g(R)dT^2 + g(R)^{-1}dR^2 + R^2 d\Omega_{D-2}^2, \tag{4.48}$$

$$g(R) = 1 - \frac{2M}{R^2} + \frac{Q^2}{R^4} + \frac{\Lambda}{3}R^2, \tag{4.49}$$

where Λ is a cosmological constant, $\Lambda/3 \equiv 1/a^2$, M and Q are related to the Arnowitt–Deser–Misner mass m and the charge σ,

$$M = \frac{4\pi G_5 m}{3\pi^2}, \qquad Q^2 = \frac{4\pi G_5 \sigma^2}{3}. \tag{4.50}$$

and σ is the charge of the electromagnetic field (purely electric) with only one nonzero component

$$A = A_T dT = \left(-\sqrt{\frac{3}{4}} \frac{Q}{R^2} + \Phi \right) dT, \tag{4.51}$$

where Φ is the constant

$$\Phi = \frac{\sqrt{3}}{2} \frac{Q}{R_+^2}$$

and R_+ is the largest real root of $g(R)$. The thermodynamics of the charged BH is described by the grand canonical potential (free energy) $W = I/\beta$, the Hawking temperature $T = 1/\beta$, and the chemical potential [37, 38] given by

$$I = \frac{\pi\beta}{8G_5 a^2}\left(a^2 R_+^2 + R_+^4 - \frac{Q^2 a^2}{R_+^2} \right), \qquad T = \frac{1}{4\pi}g'(R_+), \qquad \mu = \frac{\sqrt{3}Q}{2R_+^2}, \tag{4.52}$$

where R_+ is the outer horizon, $g(R_+) = 0$, and I is given by the value of the action at (4.49) and (4.51). The relation to the first law of thermodynamics, $d\mathscr{E} = T\,d\mathscr{S} + \mu\,d\mathscr{Q}$, is obtained under the identifications

$$W = \mathscr{E} - T\mathscr{S} - \Phi\mathscr{Q}, \qquad \mathscr{E} = m, \qquad \mathscr{S} = \frac{S_H}{4G_5}, \qquad \mathscr{Q} = q, \qquad \mu = \Phi. \tag{4.53}$$

We note that just the asymptotic value of a single gauge field component gives the chemical potential [39]–[42]

$$\mu = \lim_{r \to \infty} A_t(r). \tag{4.54}$$

The QGP is characterized at least by two parameters: the temperature and the chemical potential. Generally speaking, quantum field theories can have nonzero chemical potentials for any or all of their Noether charges. In the AdS/CFT context, two different types of chemical potential are considered: related to the R-charge and to the baryon number.

The baryon number charge can only occur when we have a theory containing fundamental flavors. Introducing flavors into the gauge theory via a D7 brane leads to the appearance of a $U(N_{\text{f}})$ global flavor symmetry. The flavor group contains $U(1)_{\text{B}}$, i.e., a baryon number symmetry, and a chemical potential μ_{B} is added for this baryon number [43]. To calculate the free energy, we must calculate the Dirac–Born–Infeld action for a D7 brane. We note that there is a divergence in the formal definition, and we must hence go through the renormalization process (see, e.g., the lectures in [44] and also see [27]).

5. Holographic Thermalization

5.1 BH formation in AdS. General

By thermalization of some class of space-time geometries we mean that space-time geometries without an event horizon evolve to space-times with an event horizons. In particular, we can consider geometries of deformed AdS space-times (space-times that are asymptotical AdS) and ask under which conditions they evolve to the AdS space with a black hole, or black branes. We have the following picture of geometry evolutions in asymptotically AdS spaces.

- The Schwarzschild AdS is an equilibrium "point" in a space of asymptotically AdS space-times geometries, the point BH AdS in Fig.5.A.

- Black branes AdS are stable under "some fluctuations" (constrained equilibrium) and other fluctuations push them to evolve to black brane configurations, the point BB AdS in Fig.5. A.

- AdS is stable under small fluctuations and is unstable under large nonlinear fluctuations, the point AdS in Fig.5.A. The picture in the circle AdS in Fig.5.A. schematically represents large chaotic deformations.

Let us first make more comments about pictures presented in Fig.5 and then give them an interpretation within the AdS/CFT dual approach. Note that these pictures are based on conjectures, supported by numerical calculations.
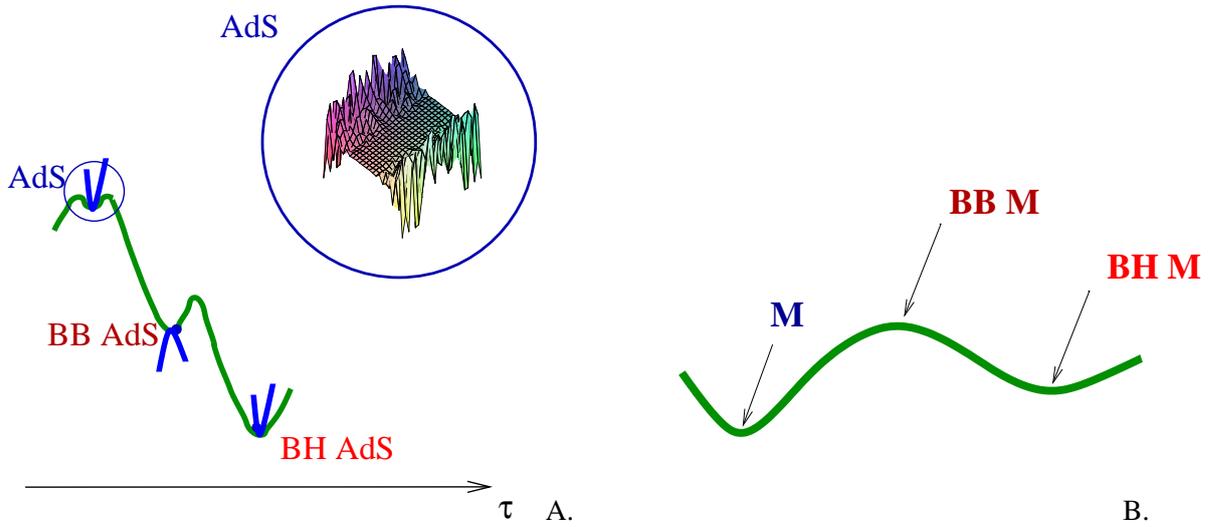
Figure 5: Schematics pictures of deformations of the AdS space-time (A) and the Minkowski space-time (B). A. Blue curves near points AdS, BB AdS (black brane in AdS) and BH AdS (black hole in AdS) show deformations in different directions. The picture in the circle A schematically represents chaotic deformations. B. A schematical picture of asymptotically Minkowski space-times geometries with black holes (BH M) and black branes (BB M).

The picture presented in Fig. 5.A radically differs from the picture in Fig. 5.B, describing situation in the Minkowski space-time. The point M is stable under rather "large" fluctuations, since the Minkowski space is stable under finite perturbations [45, 46]. But this is not so in AdS. AdS might be nonlinearly unstable to transferring energy to smaller and smaller scales and eventually forming a small black hole [47, 48, 49, 50, 51]. This is considered as a turbulence instability of AdS. One can say that after a sufficiently long time, any finite excitation of AdS eventually finds itself inside its Schwarzschild radius and collapses to a black hole.

The decay of small perturbations of an AdS black brane/black hole geometry (deformations near the points BB AdS and BH AdS) are well studied. In particular, the quasi-normal modes of fields propagating in the black brane background are studied [52]-[58]. In the context of dual approach to relativistic heavy-ion collisions, this is relevant for the study of viscous corrections to hydrodynamics and other transport processes in the presence of a thermal gauge theory plasma (see e.g. [59] for a review).

The gravitational collapse of matter injected into Minkowski space-time and the formation of an event horizon are old problems in general relativity [60, 61, 62]. One can ask the same question in AdS and investigate what deformations of AdS metric ends up by the BH formation.

In the context of AdS/CFT we interesting to deformations that can be interpreted as dual to the initial state of a relativistic heavy-ion collision, which contains two highly energetic nuclei, and therefore these deformation have to inject energy into the AdS geometry at high momentum or short distance scales. Examples of such deformations are

- colliding gravitational shock waves [63]-[75],

- drop of a shell of matter with vanishing rest mass ("null dust") [76]-[82]

- sudden perturbations of the metric near the boundary that propagate into the bulk [83, 84]

The interesting question is how long is the time of BH formation. This question has a particular interest for plasma formation within AdS/CFT.

In [50, 51] was concludes that BH formation occurs very rapidly, close to the causal bound for a very wide range of black hole masses.

In this context let us mention the previous works studied the gravitational collapse in AdS_{d+1} and also estimated the time of collapse, see [84] and refs therein. The counterpart to Chandrasekhar limit for a gravitational collapse of a degenerate star to a black hole in AdS/CFT has been investigated in [85]. Appearance of EH due to change in couplings or other background fields than the bulk metric has studied [86, 87].

Advantages of two first cases listed above that one can perform at list a part of estimations analytically. We consider these estimations in the next two sections.

6. BH formation in AdS in collision of shock waves

6.1 Shock waves in AdS_5

Shock waves propagating in the AdS space have the form [91]-[96]

$$ds^2 = L^2 \frac{-du\,dv + dx_\perp^2 + \phi(x_\perp, z)\delta(u)\,du^2 + dz^2}{z^2}, \tag{6.1}$$

where u and v are light-cone coordinates and $x_\perp$ is the coordinate transverse to the direction of motion of the shock wave and to the z direction. This metric is sourced by the stress–energy–momentum tensor T_{MN} with only one nonzero component T_{uu}^{SW},

$$T_{uu}^{\text{SW}} = J_{uu}(z, x_\perp)\delta(u). \tag{6.2}$$

and the Einstein equation of motion reduces to

$$\left(\Box_{H_3} - \frac{3}{L^2}\right)\Phi(z, x_\perp) = -16\pi G_5 \frac{z}{L} J_{uu}(z, x_\perp), \tag{6.3}$$

where

$$\Phi(z, x_\perp) \equiv \frac{L}{z}\phi(z, x_\perp) \tag{6.4}$$

and

$$\Box_{H_3} = \frac{z^3}{L^2}\frac{\partial}{\partial z} z^{-1}\frac{\partial}{\partial z} + \frac{z^2}{L^2}\left(\frac{\partial^2}{\partial x_\perp^2}\right). \tag{6.5}$$

Different forms of the shock waves correspond to different forms of the source $J_{uu}(z, x_\perp)$. The most general $O(3)$-invariant shock wave in the AdS space located at $u = 0$ corresponds to

$$\Phi^{O(3)}(z, x_\perp) = F(q), \tag{6.6}$$

where q is the chordal distance

$$q = \frac{(x_\perp^1)^2 + (x_\perp^2)^2 + (z - z_0)^2}{4zz_0}, \tag{6.7}$$

In this case ρ, related to J_{uu} as

$$\frac{z}{L} J_{uu}(z, x_\perp) \equiv \rho(z, x_\perp), \tag{6.8}$$

has the form

$$\rho^{O(3)}(z, x_\perp) = \rho(q), \tag{6.9}$$

and the Einstein equation of motion becomes

$$\left(\Box_{H_3} - \frac{3}{L^2} \right) F = -16\pi G_5 \rho(q) \tag{6.10}$$

or, explicitly,

$$q(q+1)F''_{qq} + (3/2)(1+2q)F'_q - 3F = -16\pi G_5 L^2 \rho(q). \tag{6.11}$$

Point shock wave

The point shock wave shape F^{p} is given by the solution of (6.3) with

$$J_{uu} = E\delta(u)\delta(z-L)\delta(x^1)\delta(x^2) \tag{6.12}$$

and has the form

$$F^{\mathrm{p}}(z, x_\perp) = \frac{8L^2 G_5 E z^3}{(x_\perp^2 + (z-L)^2)^3}. \tag{6.13}$$

This point shock wave shape is in fact equal to $F^{\mathrm{p}}(q)$, $\Phi^{\mathrm{p}}(z, x_\perp) = F^{\mathrm{p}}(q)$, which is a solution of (6.11) with

$$\rho^{\mathrm{p}}(q) = \frac{E}{L^3} \frac{\delta(q)}{\sqrt{q(1+q)}}. \tag{6.14}$$

It has the form

$$F^{\mathrm{p}} = \frac{2G_5 E}{L} \left(\frac{(8q^2 + 8q + 1) - 4(2q+1)\sqrt{q(1+q)}}{\sqrt{q(1+q)}} \right). \tag{6.15}$$

Charged point shock wave

The shape of the charged point shock wave is a sum of two components

$$F = F^{\mathrm{p}} + F^Q, \tag{6.16}$$

where F^{p} is given by (6.15) and F^Q is the solution of (6.11) with

$$\rho^{\mathrm{p}Q} = \frac{5\bar{Q}^2}{32 \cdot 64 L^5 G_5} \frac{1}{[q(q+1)]^{5/2}} = \frac{5Q_n^2}{\pi 24 \cdot 64 L^5} \frac{1}{[q(q+1)]^{5/2}} \tag{6.17}$$

or, explicitly,

$$F^Q = \frac{5G_5 Q_n^2}{48 L^3} \frac{144q^2 + 16q - 1 + 128q^4 + 256q^3 - 64(2q+1)q(q+1)\sqrt{q(1+q)}}{q(1+q)\sqrt{q(1+q)}}. \tag{6.18}$$

More complicated shock waves in AdS were considered in [92]-[97].

Plane shock wave

A much simpler dual description of the colliding nuclei using a wall-on-wall collision in the bulk was proposed in [68]. The Einstein equation for the profile of the wall shock wave [68] has the form

$$\left(\partial_z^2 - \frac{3}{z}\partial_z\right)\phi(z) = J_{uu}^{\text{WP}}, \qquad J_{uu}^{\text{WP}} = -16\pi G_5 \frac{E}{L^2} \frac{z_0^3}{L^3}\delta(z-z_0). \tag{6.19}$$

However, the wall shock wave approach requires a special attention to the regularization problem, since the trapped surface is assumed to be smooth and compact by definition, while the solution in [68] is nonsmooth and noncompact, see [75] for discussion of this problem.

6.2 Multiplicity and GYP dual conjecture

Gubser, Yarom, and Pufu (GYP) proposed the following holographic picture for colliding nuclei dual to QCD [63]:

- the bulk dual of the boundary nuclei is the shock waves of form (6.1) propagating in the AdS space;

- the bulk dual of two colliding nuclei in the bulk is the line element for two identical shock waves propagating towards one another in the AdS space,

$$ds^2 = L^2 \frac{-du\,dv + dx_\perp^2 + \phi_1(x_\perp, z)\delta(u)\,du^2 + \phi_2(x_\perp, z)\delta(v)\,dv^2 + dz^2}{z^2}; \tag{6.20}$$

- when the shock waves collide in the bulk, a BH should form, signifying the formation of a QGP.

The TS technic [62, 98] is usually used to estimate the BH formation.[1] A TS is a surface whose null normals all propagate inward [60]. There is no rigorous proof that the TS formation in the asymptotically AdS space–time provides the BH formation, but there is a common belief that TSs must lie behind an event horizon and that a lower bound on the entropy S_{AdS} of the BH is given by the TS area A_{trapped},

$$S_{\text{AdS}} \geq S_{\text{trapped}} \equiv \frac{A_{\text{trapped}}}{4G_5}. \tag{6.21}$$

The relations between the bulk parameters G_5, L, and E and the QGP phenomenological parameters must be fixed to make the proposed duality prescription more precise. According to [63], one of these relations is

$$\frac{L^3}{G_5} = \frac{16E \cdot T^4}{3\pi^3} = \frac{11 \cdot 16}{3\pi^3} \approx 1.9. \tag{6.22}$$

The arguments supporting (6.22) are as follows. Lattice calculations for the QGP in [17] showed that ET^4 is a slowly varying quantity and

$$\frac{E}{T^4} \approx 11. \tag{6.23}$$

---

[1]This estimate can be also obtained using the so-called capture arguments [99, 97].

Just to match BH equation of state (4.41) to (6.23), GYP assumed (6.22) (see [63]). It is important that an identification of the total energy of each nucleus with the energy of the corresponding shock wave is assumed here. We can modify this identification and assume that only a part of the gravitational shock wave energy is related to the total energy of the nucleus.

The AdS/CFT dual relation (4.44) between the expectation value of the gauge theory stress tensor and the AdS$_5$ metric deformation by the shock wave was used in [63] to fix the dimensionless parameter EL:

$$\langle T_{uu} \rangle = \frac{L^2}{4\pi G_5} \lim_{z \to 0} \frac{1}{z^3} \Phi(z, x_\perp) \delta(u). \tag{6.24}$$

For the point shock wave Φ^{p} given by (6.13), we obtain the stress tensor in the boundary field theory

$$\langle T_{uu} \rangle = \frac{2L^4 E}{\pi (L^2 + (x^1)^2 + (x^2)^2)^3} \delta(u). \tag{6.25}$$

The right-hand side of (6.25) depends on the total energy E and L, and L has the meaning of the root-mean-square radius of the transverse energy distribution. It was assumed in [63] that L is equal to the root-mean-square transverse radius of the nucleons, which in accordance with a Woods–Saxon profile for the nuclear density [100, 101] is of the order of a few fm. In particular, it is equal to $L \approx 4.3$ fm for Au and $L \approx 4.4$ fm for Pb.

The RHIC collides Au nuclei (A=197) at $\sqrt{s_{NN}} = 200$ GeV. This means that each nucleus has the energy $E = 100$ GeV per nucleon, for a total of about $E = E_{\mathrm{beam}} = 19.7$ TeV for each nucleus.

The LHC will collide Pb nuclei (A=208) at $\sqrt{s_{NN}} = 5.5$ TeV, which means $E = E_{\mathrm{beam}} = 570$ TeV.

The estimates in [63] for the dimensionless values EL for Au-Au and Pb-Pb collisions are

$$EL\big|_{\mathrm{Au-Au}, \sqrt{s_{NN}}=200\,\mathrm{GeV}} \approx 4.3 \times 10^5, \tag{6.26}$$

$$EL\big|_{\mathrm{Pb-Pb}, \sqrt{s_{NN}}=5.5\,\mathrm{TeV}} \approx 1.27 \times 10^7. \tag{6.27}$$

We note that tuning the scale L or z_0 of the bulk colliding object to the size of the nucleus or to the "saturation scale" Q_s in the "color glass" models was proposed in [68].

The calculations in [63] show that in the limit of a very large collision energy E, the entropy increases as $E^{2/3}$,

$$S_{\mathrm{trapped}} \approx \pi \left(\frac{L^3}{G_5} \right)^{1/3} (2EL)^{2/3}. \tag{6.28}$$

Considering off-center collisions of gravitational shock waves in the AdS space do not change the scaling $E^{2/3}$. But a critical impact parameter, beyond which the TS does not exist, was observed in [68] (cf. the result in [66]). Experimental indications for a similar critical impact parameter in real collisions had been noted [68].

The relation of the total multiplicity S_{QGP} (given by experimental data) to the entropy S_{AdS} produced in the gravitational wave collision in AdS$_5$ has some subtleties [63]. Phenomenological considerations [102, **?**, 63] lead to estimating the total multiplicity S_{QGP} by the number N_{ch} of charged particles times a factor ~ 7.5,

$$S_{\mathrm{QGP}} \approx 7.5 N_{\mathrm{ch}}. \tag{6.29}$$

(a)   (b)
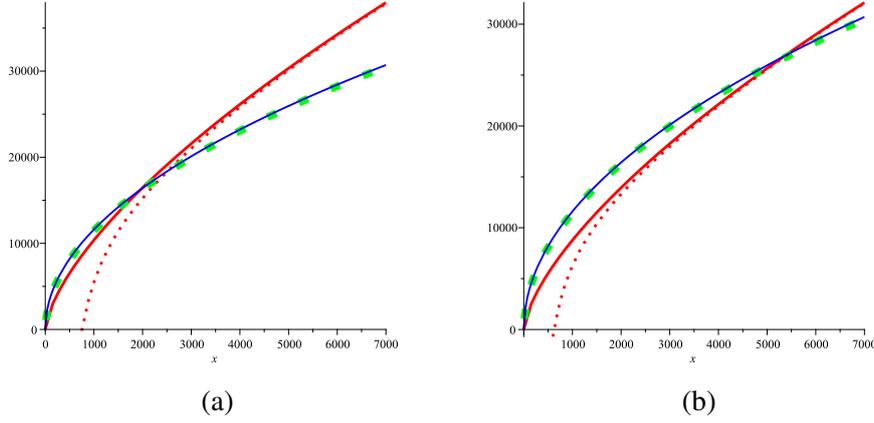
Figure 6: (color on-line) Plots of the total number of charged particles versus energy: the red lines represent estimate (2.45). The plots in (a) and (b) differ by the overall factor $\mathcal{M}$. The blue lines correspond to the prediction of the Landau model, and the dotted green lines schematically represent the curves that fit the experimental data. The dashed lines correspond to corrections to the GYP multiplicity via a nonzero chemical potential (see Sect. 3).

The TS analysis does not give the produced entropy, but it provides a lower bound,

$$S_{\text{trapped}} \leq S_{\text{AdS}}. \tag{6.30}$$

Taking into account that in the calculations in [63], the gravitational shock wave energy was identified with the energy of colliding ions and L was identified with the nucleus size, we can introduce proportionality constants between these quantities and obtain

$$\mathcal{M} \cdot S_{\text{trapped}} < N_{\text{ch}}, \tag{6.31}$$

where all proportionality factors are included in the overall factor $\mathcal{M}$. We can take $\mathcal{M}$ to fit the experimental data at some point. But the scaling $S_{\text{trapped}} \propto s_{NN}^{1/3}$ implied by (6.28) differs from the observed scaling, which is closer to the dependence $S \propto s_{NN}^{1/4}$, which is predicted by the Landau model [33] (see Fig. 6). Obviously, we can avoid a conflict between [63] and the experiment if $E < E_{\text{max}}$, but if E can be arbitrary large, then the conflict arises.

In Fig. 6, we plot the dependence of entropy bound (6.28) on the energy together with the curve schematically representing the realistic curve that fits the experimental data [103]. It can be seen that by changing the coefficient $\mathcal{M}$, we can avoid the conflict only for energy up to some E_{max}. We chose the overall coefficient of the numerical plot to fit the RHIC data [103], which are indicated by dots in Fig. 6.

In the above estimate, the energy of each shock wave is identified with the energy of colliding beams. As was noted in [64], the fit to the data can be improved by identifying the energy of each shock wave with the fraction of the energy of the nucleus carried by a nucleus participating in the collision. This gives an extra parameter for fitting the data. But a conflict still arises at high energies. It was proposed in [64] to solve this problem by removing a UV part of the AdS bulk. Shock waves corresponding to the BH with a nonzero dilaton field [104] were considered in [73], where it was shown that the lower bound on N_{ch} scales is closer to $s_{NN}^{1/4}$.

7. BH formation in AdS by falling shell

The $(d+1)$-dimensional infalling matter shell in *AdS* in Poincaré coordinates is described by the Vaidya metric

$$ds^2 = \frac{1}{z^2}\left[-\left(1 - m(v)z^d\right)dv^2 - 2dz\,dv + d\mathbf{x}^2 \right], \tag{7.1}$$

where v is the null coordinate, $\mathbf{x} = (x_1, \ldots, x_{d-1})$ are the spatial coordinates on the boundary $z = 0$ and we have set the AdS radius equal to 1. We take $m(v)$ in the form

$$m(v) = M\theta(v), \tag{7.2}$$

where M is a constant and $\theta(v)$ is the Heaviside function. This function can be regularized as

$$m(v) = \frac{M}{2}\left(1 + \tanh\frac{v}{\mu}\right), \tag{7.3}$$

μ characterizes the thickness if the shell at the point $v = 0$. One gets (7.2) from (7.3) under $\mu \to 0$.

For $m(v) = M$ the change of variables

$$dv = dt - \frac{dz}{1 - M z^d} \tag{7.4}$$

brings (7.1) to the standard metric of the black hole in *AdS* in the Poincare coordinates

$$ds^2 = \frac{1}{z^2}\left[-\left(1 - Mz^d\right)dt^2 + \frac{dz^2}{1 - Mz^d} + d\mathbf{x}^2 \right]. \tag{7.5}$$

For $v < 0$ the metric (7.1) with $m(v)$ in the form (7.2) is just the *AdS* metric.

For metrics (7.1),(7.2) for $d = 2, 3, 4$ the geodesics, stated and ended on the boundary at points $(-l/2, t_0, 0)$ $(l/2, t_0, 0)$, respectively, are studied in papers [105, 79, 77, 78, 80]. In this calculations the regularization $(\pm l/2, t_0, 0) \to (\pm l/2, t_0, z_0)$ has been used, here z_0 is the parameter of the ultaviolet cut-off (compare with [27]). For AdS_3 the renormalized length is $\delta\mathscr{L} = 2\ln(l/2)$.

The length of geodesic relating points in AdS_3 $(\pm l/2, t_0, z_0)$ and crossing the shell (see Fig. 7.B) is given by the parametrical formula [77, 78, 80]

$$\delta\mathscr{L}(t_0, \ell) = 2\ln\left[\frac{\sinh(r_H t_0)}{r_H s(\ell, t_0)}\right], \tag{7.6}$$

here $s(\ell, t_0) \in [0, 1]$ is a parameter defined from the condition

$$\ell = \frac{1}{r_H}\left[\frac{2c}{s\rho} + \ln\left(\frac{2(1+c)\rho^2 + 2s\rho - c}{2(1+c)\rho^2 - 2s\rho - c}\right)\right] \tag{7.7}$$

è

$$2\rho = \coth(r_H t_0) + \sqrt{\coth^2(r_H t_0) - \frac{2c}{c+1}}. \tag{7.8}$$

here $s = \sqrt{1 - c^2}$, $\rho = 1/(r_H z_c)$, $r_H = \sqrt{M}$, z_c is a coordinate of the shell crossing point, c is an arbitrary parameter less then 1. It is clear that for any ℓ, for a time large enough the geodesic related

the points $(\pm \vec{l}/2, t_0, z_0)$ will become inside the black hole, see Fig.7.C, and in this case the geodesic length is given by the expression

$$\delta\mathscr{L}_{thermal}(\ell) = 2\ln[\frac{1}{r_H}\sinh r_H \ell/2], \tag{7.9}$$

that means the thermalization for large enough ℓ. For later times the geodesic length does not change, see Fig.7.D.
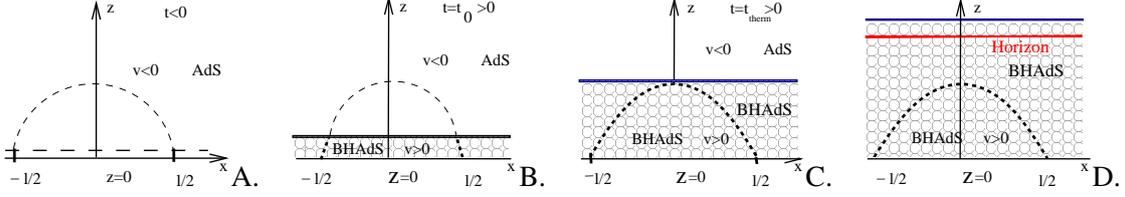
Figure 7: Cartoon of the process describing the appearance of the black hole. A. The geodesic is in the empty AdS space; the horizontal line images the regularization. B. The geodesic connected points $\pm l/2$ is partially in the black hole region. C. The same geodesic is totally in the black hole region. D. The geodesic is in the black hole region in all later times

To describe the Hawking radiation we can use the Vadya *AdS* metric with negative energy (with negative mass function), compare with [106]. The process of evaporation of the black hole is presented in Fig.8 and the process of creation of the black hole and the subsequence radiation is presented in Fig.9.
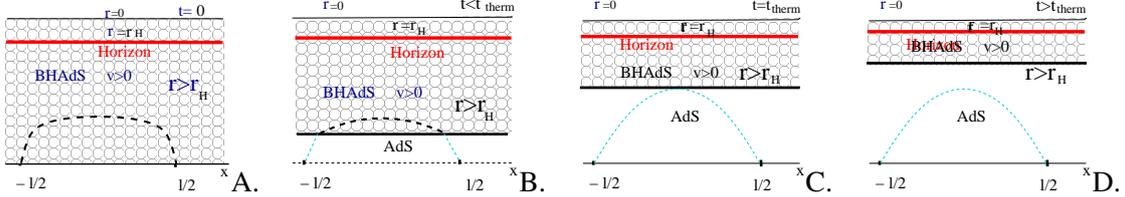
Figure 8: Cartoon of the black hole evaporation: A. The geodesic connected points $\pm l/2$ is totally in the black hole region. B. A partial evaporation of the black hole from the point of view of two points $\pm \vec{\ell}/2$ correlator, i.e. the geodesic is partially in the black hole region. C. The total evaporation of the black hole from the point of view of this correlator, i.e. the geodesic totally abandons the black hole region. D. The geodesic is totally in the empty region in all subsequent momenta of time.

The metric of this process is given by the formula (7.1) with $m(v)$

$$m(v) = M\theta(v) - M_1\theta(v - v_1), \tag{7.10}$$

The case of the full determalization corresponds to $M = M_1$ and will be considered in what follows. If the distance ℓ is essential less then v_1, then in the given moment of time the geodesic cross no more then 2 point of the shell. This case is schematically presented in Fig.8. As we can see form the figures, for $0 < t < v_1$ the length of the geodesic connected the points $(\pm l/2, t_0, z_0)$ and crossing the shell (see Fig. 7. B) is given by formula (7.6), (7.7) and (7.8). Then the length of the
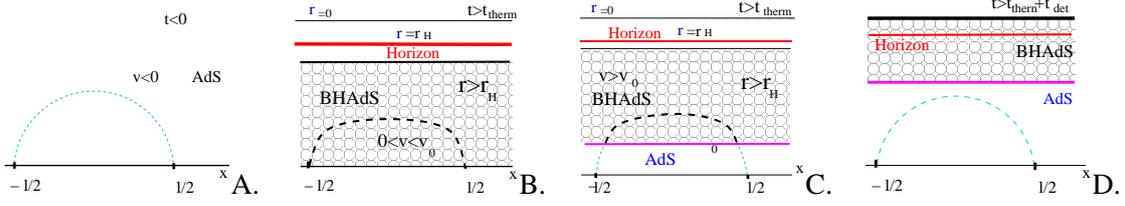
Figure 9: Cartoon of the black formation and the subsequent black hole evaporation: transition from A to B shows the black hole creation; C shows the black hole evaporation and D shows the total black hole evaporation.

geodesic does not change till $t^* < t < v_1$, Fig.8. B. Starting from $v_1 = t$ the geodesic crosses the shell at 2 points, Fig.8. C, and the length of the geodesic is given by new (as compare with (7.6), (7.7)) formula. These formula we obtain considering relations between the change of the value of the affine paremeter and the value of the change of the coordinate x on the different part of the geodesic. These relations have the form

$$
\begin{aligned}
l &= l_{AdS,1} + l_{AdS,2} + l_{BHAdS,1} + l_{BHAdS,2} \\
&= \frac{4}{p_x r_c}\left(r_c - \sqrt{r_c^2 - p_x^2}\right) - 2p_x^2 \ln\left(\frac{r_t^2(2 - r_c^2 G_+ + 2\sqrt{F(r_c)})}{r_c^2(2 - r_t^2 G_+ + 2\sqrt{F(r_t)})}\right)
\end{aligned}
\tag{7.11}
$$

è

$$
\begin{aligned}
L_{ren} &= \delta L_{ren} + L_{AdS,1} + L_{AdS,2} + L_{BHAdS,2} + L_{BHAdS,2} \\
&= -4\log(r_c + \sqrt{r_c^2 - p_x^2}) + \ln\left(\frac{-(p_x^2 + 1 - E_B^2) + 2r_c^2 + 2\sqrt{D(r_c)}}{-(p_x^2 + 1 - E_B^2) + 2r_t^2 + 2\sqrt{D(r_t)}}\right)
\end{aligned}
\tag{7.12}
$$

here *ren* means the renormalized length and the following notations are introduced

$$
G_+ = p_x^2 + 1 - E_B^2, \quad G_- = -p_x^2 + 1 + E_B^2
\tag{7.13}
$$

$$
D(r) = r^4 + (E_B^2 - 1 - p_x^2)r^2 + p_x^2
\tag{7.14}
$$

$$
F(r) = p_x^2 r^4 - (p_x^2 + 1 - E_B^2 p_x^2)r^2 + 1
\tag{7.15}
$$

and we consider the case when in the empty *AdS* space the geodesic has zero energy (the case of nonzero energy corresponds to non-equal time correlator), and the energy in the black space (in *BHAdS* space) is defined from the refraction condition

$$
E_B = -\frac{1}{2r_c^2}\sqrt{r_c^2 - p_x^2}.
\tag{7.16}
$$

here r_c is the coordinate of the crossing point, p_x is the angular momentum that is the integral of motion and has no a junction under crossing the geodesic (as opposed to the energy, that has according to (7.16) a junction under a crossing of the shell), r_t is the turning point of the geodesic. We have a relation

$$
r_{t\pm}^2 = \frac{(1 + p_x^2 - E_B^2) \pm \sqrt{(1 + p_x^2 - E_B^2)^2 - 4p_x^2}}{2}
\tag{7.17}
$$

22

Let us clarify the meaning of (7.11), (7.13), (7.16) and (7.17). Here r_c is a free parameter that specifies the position of the shell, p_x is a parameter that does not change in shell moving, E_B is given by (7.16), and r_t given by formula (7.17). Therefore, under r_c and p_x fixed, formula (7.11) and (7.13) give the relation between renormalized geodesic length L_{ren} and the distance l.

As it is seen from 8.D, starting from $t \geq t_1^*$ the geodesic related the points $(\pm l/2, t_0, z_0)$ occurs totaly outside the black hole and the geodesic length will be given by formula $\delta \mathscr{L} = 2 \ln(\ell/2)$.

In [21] it has been proposed to estimate the ratio of the thermalization time over the freeze-out time using a holographic AdS-Vaidya model. In the model the freeze-out is described as the black hole evaporation due to the Hawking radiation that is modeled by the Vaidya metric with a negative mass.

Let us consider the AdS-Vadiya metric (7.1) with

$$m(v) = M(\theta(v) - \theta(v - v_1)), \tag{7.18}$$

where $M > 0$ and v_1 is larger than the thermalization time, $v_1 > t_{ther}$.

Let us suppose that the vector $\vec{l}$, characterizing the equal times two points on the boundary, at which the geodesic states and ends, has only one nonzero component, $l_1 \equiv \ell$, and denote $J_1 = J$. The thermalization time for the correlation function at for these two points is given by

$$\tau_{therm} = \int_J^\infty \frac{dr}{r^2 \left(1 - \frac{M}{r^d}\right)}, \tag{7.19}$$

here J is the first component of the conserved angular momentum related with ℓ

$$\ell = 2J \int_J^\infty \frac{dr}{r^2 \sqrt{(r^2 - J^2)\left(1 - \frac{M}{r^d}\right)}}. \tag{7.20}$$

From these formulas we get that

$$\frac{\tau_{ther}}{\ell} = F(m^2, d), \tag{7.21}$$

where $m^2 = M/J^d \rho^d$ and $F(m^2, d)$ is given by

$$F(m^2, d) = \frac{\int_1^\infty \frac{d\rho}{\rho^2 \left(1 - \frac{m^2}{\rho^d}\right)}}{2 \int_1^\infty \frac{d\rho}{\rho^2 \sqrt{(\rho^2 - 1)\left(1 - \frac{m^2}{\rho^d}\right)}}}. \tag{7.22}$$

Now, in the 4-dimensional Minkowski space, i.e. for $d = 4$ for the function $F(m^2, 4)$ as a function of m, $0 < m < 1$, we have the bound

$$0.39 \leq F(m^2, 4) \leq 0.5, \tag{7.23}$$

see Fig.10. Therefore we obtain the bound for the thermalization time (d=4)

$$0.39 \leq \frac{\tau_{ther}}{\ell} \leq 0.5, \tag{7.24}$$

The similar bounds take place for other $d > 2$ [77, 79, 80].

The dethermalization time, under assumption that $v_1 > \tau_{th}$ and for the same points on the boundary, is defined by the formulas (7.19) and (7.20) with $M = 0$. Since $F(0,d) = 1/2$ we have

$$\frac{\tau_{det}}{\ell} = \frac{1}{2} \tag{7.25}$$

Note, that (7.25) does not depend on the space time dimension d.

From (7.24), (7.25) we obtain the following relation between thermalization and dethermalization times for observables at the same distance:

$$0.78 < \frac{\tau_{ther}}{\tau_{det}} < 1 \tag{7.26}$$

We see that this ratio is universal and does not depend on the distance between two points till the distance is less then v_1.

Therefore, the minimal ratio of thermalization time to determalization time, that can be realized in the $d = 4$ AdS-Vadiya model is 0.78. Increasing d one gets a possibility to decrease this ratio, see 10.B. As it has been noted in [81, 82] involving the nonzero chemical potential one increases the ratio of τ_{therm} to ℓ, and therefore, in our model, this increases τ_{therm}/τ_{der}. One can also try to add by hands an effective locking potential, for example, the quadratic one. This corresponds to a change $(1 - m^2/\rho^d) \to (1 - m^2/\rho^d + q\rho^2)$ in (7.22). This locking potential decreases the ratio $F(m,q,4) = \tau_{therm}/\tau_{der}$, see Fig.10.C.

It is known that the experimental data on heavy ion collisions determine the thermalization time as $\tau_{ther} \sim 1$ fm/c and the dethermalization time as $\tau_{det} \sim 10 - 20$ fm/c, so $\tau_{ther}/\tau_{det} \sim 0.1 - 0.05$. It seems at the first sight that it is difficult to explain this data using our model. This is in fact so, if one thinks that thermalization and the dethermalization have to be happen at the same scale, but it is not so if the scales of thermalization and the dethermalization are different. For the thermalization time, the relevant length scale according [77] can be taken about $\ell \sim 0.6$ fm, that is the thermal scale $l \sim \hbar/T$ for the temperature value $T \sim 300 - 400 MeV$ at heavy ion collider energies, and one obtains the estimate $\tau_{therm} \sim 0.3$fm/c, which is smaller then the experimental data.

One can fit better the experimental data using the scale $l \sim 2$ fm. One of possible explanations of this scale is a classical estimation of the distance between the nucleons inside the nucleus. One gets this estimation by taking into account that the radius of the nucleus of Pb is about $r_{Pb} \approx 7$ fm, and in the sphere with this radius one can pack 208 (A=208 for Pb) balls with radius

$$r_n = \sqrt[3]{\frac{\eta_K}{208}} \, r_{Pb} \approx 1.07 \, \text{fm}. \tag{7.27}$$

Here η_K is the Kepler number $\eta_K = \pi/\sqrt{18} \approx 0.74$. From this consideration it seems natural to take $l = 2r_n \sim 2$ fm as a typical scale of the thermalization. In this case one has $\tau_{therm} \sim 1$ fm/c.

For an estimation of the dethermalization time, one can take as the typical scale the size of the nucleus, i.e. $l_{det} \sim 2r_{Pb} \sim 14$ fm. Then one gets the dethermalization time $\tau_{det} \sim 7$fm/c. Note that this estimation gets a low bound, since in the model we have the free parameter v_1. For the ratio one gets

$$\frac{\tau_{ther}}{\tau_{det}} = \frac{\tau_{ther}}{0.5 \cdot l_{ther}} \cdot \frac{l_{ther}}{l_{det}} = 0.39 \cdot \frac{2}{14} \approx 0.056, \tag{7.28}$$
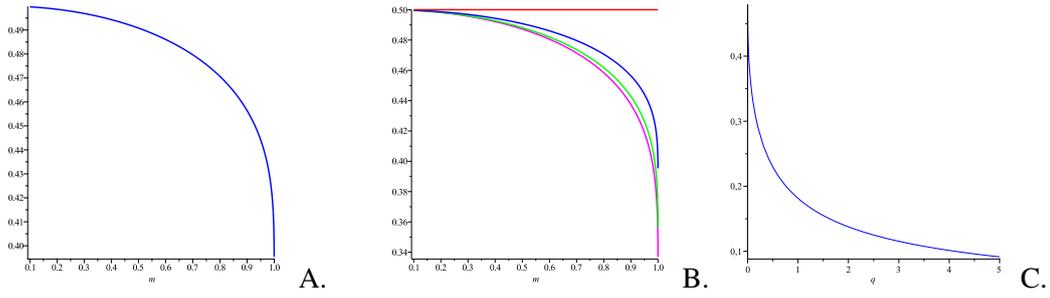
Figure 10: A. The plot of $F(m^2, 4)$ as function of m. B. The plot shows the dependence of the below bound of $F(m^2, d)$ on dimension d. d=2 corresponds to the red line, d=4,6,8 to blue, green and magenta lines, respectively. C. The plot of $F(m^2, q, 4)$ as function of q and $m^2 = 0.99$.

which is in agreement with the experimental data.

References

[1] J. Adams *et al.* [STAR Collaboration], Nucl. Phys. A **757**, 102 (2005) [arXiv:nucl-ex/0501009].

[2] K. Adcox *et al.* [PHENIX Collaboration], Nucl. Phys. A **757**, 184 (2005) [arXiv:nucl-ex/0410003].

[3] See the contributions on elliptic flow at the LHC in the proceedings of Quark Matter 2011: J. Phys. GG **38**, v 12 (2011).

[4] E. Shuryak, Prog. Part. Nucl. Phys. **53**, 273 (2004) [arXiv:hep-ph/0312227].

[5] E. Shuryak, Nucl. Phys. A **750**, 64 (2005) [arXiv:hep-ph/0405066].

[6] U. W. Heinz, "Concepts of heavy ion physics," hep-ph/0407360.

[7] C. A. Salgado, "Lectures on high-energy heavy-ion collisions at the LHC," arXiv:0907.1219 [hep-ph].

[8] F. Gelis, J. Phys. Conf. Ser. **381**, 012021 (2012) [arXiv:1110.1544 [hep-ph]].

[9] R. Snellings, New J. Phys. **13**, 055008 (2011) [arXiv:1102.3010 [nucl-ex]].

[10] M. Gyulassy and L. McLerran, Nucl. Phys. A **750**, 30 (2005); [arXiv:nucl-th/0405013].

[11] M.G. Alford, A. Schmitt, Andreas, K. Rajagopal, T. Schaefer, A. Schmitt (2008). Review of Modern Physics 80 (4): 1455Ű1515; arXiv:0709.4635

[12] E. Iancu, "QCD in heavy ion collisions," arXiv:1205.0579 [hep-ph].

[13] J. M. Maldacena, Adv. Theor. Math. Phys. **2**, 231-252 (1998) [hep-th/9711200].

[14] S. S. Gubser, I. R. Klebanov, A. M. Polyakov, Phys. Lett. **B428**, 105-114 (1998) [hep-th/9802109].

[15] E. Witten, Adv. Theor. Math. Phys. **2**, 253-291 (1998) [hep-th/9802150].

[16] J. Casalderrey-Solana, H. Liu, D. Mateos, K. Rajagopal, U. A. Wiedemann, "Gauge/String Duality, Hot QCD and Heavy Ion Collisions," [arXiv:1101.0618 [hep-th]].

[17] F. Karsch, Lect. Notes Phys. **583** (2002) 209–249; hep-lat/0106019.

[18] E. Shuryak, Prog. Part. Nucl. Phys. **62**, 48 (2009) [arXiv:0807.3033 [hep-ph]].

[19] S. Borsanyi et al., "The QCD equation of state with dynamical quarks," arXiv:1007.2580 [hep-lat]

[20] B. Muller and A. Schafer, "Entropy creation in relativistic heavy ion collisions", 1110.2378

[21] I. Y. Arefeva and I. V. Volovich, "On Holographic Thermalization and Dethermalization of Quark-Gluon Plasma," arXiv:1211.6041 [hep-th].

[22] G. Policastro, D. T. Son, and A. O. Starinets. *Phys. Rev. Lett.*, 87:081601, 2001.

[23] P. Kovtun, D. T. Son, and A. O. Starinets. *JHEP*, 10:064, 2003.

[24] P. Kovtun, D. T. Son, and A. O. Starinets. *Phys. Rev. Lett.*, 94:111601, 2005.

[25] M. P. Heller and R. A. Janik, Phys. Rev. D **76** (2007) 025027 [hep-th/0703243 [HEP-TH]].

[26] A. Buchel, Phys. Rev. D **85** (2012) 066004 [arXiv:1110.0063 [hep-th]].

[27] I. Ya. Aref'eva and I. V. Volovich, Phys. Lett. B **433**, 49 (1998), hep-th/9804182.

[28] I.M.Gelf'and and G.E.Shilov, Generalized Functions, Academic press, 1963

[29] D. T. Son and A. O. Starinets, JHEP **0209**, 042 (2002), `hep-th/0205051`.

[30] V. Balasubramanian and S. F. Ross, Phys. Rev. D **61** (2000) 044007 [arXiv:hep-th/9906226].

[31] S. W. Hawking and D. N. Page, Commun. Math. Phys. 87 (1983) 577.

[32] S. S. Gubser, I. R. Klebanov, and A. W. Peet, Phys. Rev. D54 (1996) 3915–3919; hep-th/9602135.

[33] L. D. Landau, Izv. Akad. Nauk Ser. Fiz. **17**, 51 (1953) (in Russian). [English translation: *Collected Papers of L. D. Landau, edited by D. ter Haar (Gordon and Breach, New-York, 1968)*].

[34] J. D. Bjorken, Phys. Rev. D **27**, 140 (1983).

[35] C. Fefferman and C.R. Graham, in *Elie Cartan et les Mathématiques d'aujourd'hui*, Astérisque (1985) 95.

[36] A. Bernamonti and R. Peschanski, Nucl. Phys. Proc. Suppl. **216**, 94 (2011) [arXiv:1102.0725 [hep-th]].
R. A. Janik, Lect. Notes Phys. **828**, 147 (2011) [arXiv:1003.3291 [hep-th]].

[37] A. Chamblin, R. Emparan, C. V. Johnson and R. C. Myers, Phys. Rev. D **60**, 064018 (1999); arXiv:hep-th/9902170.
A. Chamblin, R. Emparan, C. V. Johnson and R. C. Myers, Phys. Rev. D **60**, 104026 (1999); arXiv:hep-th/9904197.

[38] C. S. Peca and J. P. S. Lemos, Phys. Rev. D **59**, 124007 (1999); arXiv:gr-qc/9805004.
M. Cvetic and S. S. Gubser, JHEP **9904**, 024 (1999); arXiv:hep-th/9902195.

[39] D. Mateos, S. Matsuura, R. C. Myers, and R. M. Thomson, JHEP **11** (2007) 085,; arXiv:0709.1225

[40] R. C. Myers, M. F. Paulos, A. Sinha, JHEP **0906**, 006 (2009); arXiv: 0903.1596
S. Hands, T. J. Hollowood, and J. C. Myers, JHEP **1007**, 086 (2010); arXiv:1003.5813.

[41] A. Parnachev, JHEP 02, 062 (2008); arXiv:0708.3170.

[42] J. Erdmenger, M. Haack, M. Kaminski and A. Yarom, JHEP **0901**, 055 (2009); arXiv:hep-th/0809.2488.

[43] S. Kobayashi, D. Mateos, S. Matsuura, R.C. Myers and R.M. Thomson, JHEP **0702**, 016 (2007); arXiv:hep-th/0611099.

[44] K. Skenderis, Class. Quant. Grav. 19 (2002) 5849; hep-th/0209067.

[45] D. Christodoulou, S. Klainerman, "The global nonlinear stability of the Minkowski space," Princeton University Press, Princeton, 1993.

[46] H. Friedrich, Commun. Math. Phys. **107** (1986) 587.

[47] P. Bizon and A. Rostworowski, *Phys.Rev.Lett.* **107** (2011) 031102, arXiv:1104.3702.

[48] J. Jalmuzna, A. Rostworowski and P. Bizon, Phys. Rev. D **84**, 085021 (2011) [arXiv:1108.4539 [gr-qc]].

[49] O. J. C. Dias, G. T. Horowitz and J. E. Santos, Class. Quant. Grav. **29**, 194002 (2012) [arXiv:1109.1825 [hep-th]].

[50] D. Garfinkle and L. A. Pando Zayas, Phys. Rev. D **84**, 066006 (2011); [arXiv:1106.2339 [hep-th]].

[51] D. Garfinkle, L. A. Pando Zayas and D. Reichmann, JHEP **1202**, 119 (2012), arXiv:1110.5823 [hep-th].

[52] S. Chandrasekhar and S. L. Detweiler, Proc. Roy. Soc. Lond. A **344**, 441 (1975);

[53] G. T. Horowitz and V. E. Hubeny, Phys. Rev. D **62**, 024027 (2000) [arXiv:hep-th/9909056];

[54] A. O. Starinets, Phys. Rev. **D66** (2002) 124013. [hep-th/0207133];

[55] P. K. Kovtun and A. O. Starinets, Phys. Rev. D **72**, 086009 (2005) [arXiv:hep-th/0506184];

[56] R. A. Janik and R. B. Peschanski, Phys. Rev. D **74**, 046007 (2006) [arXiv:hep-th/0606149];

[57] J. J. Friess, S. S. Gubser, G. Michalogiorgakis, S. S. Pufu, JHEP **0704** (2007) 080. [hep-th/0611005];

[58] N. Iqbal, H. Liu, Phys. Rev. **D79** (2009) 025023. [arXiv:0809.3808 [hep-th]].

[59] V. E. Hubeny and M. Rangamani, Adv. High Energy Phys. **2010**, 297916 (2010) [arXiv:1006.3675 [hep-th]].

[60] S.W. Hawking and G.R.E Ellis, The large scale structure of space–time (Cambridge Univ. Press, Cambridge, 1973).

[61] R.M. Wald, General relativity (The University of Chicago Press, Chicago, 1984).

[62] R. Penrose, unpublished, 1974.

[63] S. S. Gubser, S. S. Pufu and A. Yarom, Phys. Rev. D **78** (2008) 066014 [arXiv:0805.1551 [hep-th]].

[64] S. S. Gubser, S. S. Pufu and A. Yarom, JHEP **0911** (2009) 050 [arXiv:0902.4062 [hep-th]].

[65] D. Grumiller and P. Romatschke, JHEP **0808** (2008) 027 [arXiv:0803.3226 [hep-th]].

[66] L. Alvarez-Gaume, C. Gomez, A. Sabio Vera, A. Tavanfar and M. A. Vazquez-Mozo, JHEP **0902** (2009) 009 [arXiv:0811.3969 [hep-th]].

[67] J. L. Albacete, Y. V. Kovchegov and A. Taliotis, JHEP **0807** (2008) 100 [arXiv:0805.2927 [hep-th]].

[68] S. Lin and E. Shuryak, Phys. Rev. D **79** (2009) 124015 [arXiv:0902.1508 [hep-th]].

[69] J. L. Albacete, Y. V. Kovchegov and A. Taliotis, JHEP **0905** (2009) 060 [arXiv:0902.3046 [hep-th]].

[70] I. Y. Aref'eva, A. A. Bagrov and E. A. Guseva, JHEP **0912**, 009 (2009); arXiv:hep-th/0905.1087.

[71] I. Y. Aref'eva, A. A. Bagrov and L. V. Joukovskaya, JHEP **1003** , 002, (2010); arXiv:hep-th/0909.1294.

[72] Y. V. Kovchegov and S. Lin, JHEP **1003** (2010) 057 [arXiv:0911.4707 [hep-th]].
Y. V. Kovchegov, Prog. Theor. Phys. Suppl. **187** (2011) 96 [arXiv:1011.0711 [hep-th]].

[73] E. Kiritsis and A. Taliotis, JHEP **1204**, 065 (2012) [arXiv:1111.1931 [hep-ph]].

[74] P. M. Chesler and L. G. Yaffe, Phys. Rev. Lett. **106** (2011) 021601 [arXiv:1011.3562 [hep-th]].

[75] I. Y. Aref'eva, A. A. Bagrov and E. O. Pozdeeva, JHEP **1205**, 117 (2012), arXiv:1201.6542.

[76] U. H. Danielsson, E. Keski-Vakkuri and M. Kruczenski, Nucl. Phys. B **563**, 279 (1999).
[arXiv:hep-th/9905227].

[77] V. Balasubramanian, A. Bernamonti, J. de Boer, N. Copland, B. Craps, E. Keski-Vakkuri, B. Muller and A. Schafer *et al.*, Phys. Rev. Lett. **106** (2011) 191601 [arXiv:1012.4753 [hep-th]].

[78] V. Balasubramanian, A. Bernamonti, J. de Boer, N. Copland, B. Craps, E. Keski-Vakkuri, B. Muller and A. Schafer *et al.*, Phys. Rev. D **84** (2011) 026010 [arXiv:1103.2683 [hep-th]].

[79] J. Abajo-Arrastia, J. Aparicio and E. Lopez, JHEP 1011, 149 (2010). arXiv:1006.4090 [hep-th]

[80] R. Callan, J. -Y. He and M. Headrick, JHEP **1206**, 081 (2012), arXiv:1204.2309. .

[81] D. Galante and M. Schvellinger, JHEP **1207**, 096 (2012) [arXiv:1205.1548 [hep-th]].

[82] E. Caceres and A. Kundu, JHEP **1209**, 055 (2012) [arXiv:1205.2354 [hep-th]].

[83] P. M. Chesler and L. G. Yaffe, Phys. Rev. Lett. **102** (2009) 211601 [arXiv:0812.2053 [hep-th]]
P. M. Chesler and L. G. Yaffe, Phys. Rev. D **82** (2010) 026006 [arXiv:0906.4426 [hep-th]].

[84] S. Bhattacharyya and S. Minwalla, JHEP **0909** (2009) 034 [arXiv:0904.0464 [hep-th]].

[85] X. Arsiwalla, J. de Boer, K. Papadodimas and E. Verlinde, JHEP **1101** (2011) 144 [arXiv:1010.5784 [hep-th]].

[86] S. R. Das, T. Nishioka and T. Takayanagi, JHEP **1007** (2010) 071 [arXiv:1005.3348 [hep-th]].

[87] K. Hashimoto, N. Iizuka and T. Oka, Phys. Rev. D **84** (2011) 066005 [arXiv:1012.4463 [hep-th]].

[88] S. Lin and E. Shuryak, Phys. Rev. D **77** (2008) 085013 [hep-ph/0610168];
S. Lin and E. Shuryak, Phys. Rev. D **77** (2008) 085014 [arXiv:0711.0736 [hep-th]].

[89] G. Beuf, M. P. Heller, R. A. Janik and R. Peschanski, JHEP **0910** (2009) 043 [arXiv:0906.4423 [hep-th]].

[90] R. A. Janik, Phys. Rev. Lett. **98** (2007) 022302 [hep-th/0610144].

[91] M. Hotta and M. Tanaka, Class. Quant. Grav. **10** (1993) 307–314.

[92] K. Sfetsos, Nucl. Phys. **B436** (1995) 721–746; hep-th/9408169.

[93] G. T. Horowitz and N. Itzhaki, JHEP **02** (1999) 010; hep-th/9901012.

[94] R. Emparan, Phys. Rev. **D64** (2001) 024025; hep-th/0104009.

[95] J. Podolsky and J. B. Griffiths, Class. Quant. Grav. 15 (1998) 453–463; gr-qc/9710049.

[96] K. Kang and H. Nastase, Phys. Rev. D **72** (2005) 106003 [hep-th/0410173].

[97] I.Ya. Aref'eva, Physics of Particles and Nuclei, 41 (2010), 835, arXiv: 0912.5481.
I.Ya. Aref'eva, Inter. J. of Mod. Phys., B, Vol. 26, (2012) 1243010 (20 pp).

[98] D. M. Eardley and S. B. Giddings, Phys. Rev. D 66, 044011 (2002); arXiv:gr-qc/0201034.

[99] N. Kaloper and J. Terning, Gen. Rel. Grav. **39**, 1525 (2007) [Int. J. Mod. Phys. D **17**, 665 (2008)]; arXiv:hep-th/0705.0408.

[100] S. Klein and J. Nystrand, Phys. Rev. **C60** (1999) 014903; hep-ph/9902259.

[101] **STAR** Collaboration, J. Adams et. al., Phys. Rev. **C70** (2004) 031902; nucl-ex/0404012.

[102] S. Ochs, U. W. Heinz, Phys. Rev. **C54**, 3199-3211 (1996); hep-ph/9606458.

[103] B. B. Back et. al., Phys. Rev. Lett. **91** (2003) 052303; nucl-ex/0210015.

[104] U. Gursoy and E. Kiritsis, JHEP **0802** (2008) 032; arXiv: 0707.1324.
U. Gursoy, E. Kiritsis and F. Nitti, JHEP **0802** (2008) 019; arXiv: 0707.1349.

[105] V. E. Hubeny, M. Rangamani, T. Takayanagi, JHEP **0707** (2007) 062, arXiv:0705.0016.

[106] V. P. Frolov, I. V. Volovich, V. A. Zagrebnov, Theor.Math.Phys., 29 (1976) 1012.